PROBING DECONFINEMENT IN THE POLYAKOV-LOOP EXTENDED NAMBU–JONA-LASINIO MODEL AT IMAGINARY CHEMICAL POTENTIAL*

Kenji Morita[a], Vladimir Skokov[b,c], Bengt Friman[c]
Krzysztof Redlich[d]

[a]Yukawa Institute for Theoretical Physics, Kyoto University
Kyoto 606-8502, Japan
[b]Physics Department, Brookhaven National Laboratory, Upton, NY 11973, USA
[c]GSI Helmholtzzentrum für Schwerionenforschung, 64291 Darmstadt, Germany
[d]Institute of Theoretical Physics, University of Wrocław
pl. M. Borna 9, 50-204 Wrocław, Poland

(Received January 2, 2012)

The phase structure of Polyakov-loop extended Nambu–Jona-Lasinio (PNJL) model is explored at imaginary chemical potential, with particular emphasis on the deconfinement transition. We point out that the statistical confinement nature of the model naturally leads to characteristic dependence of the chiral condensate $\langle\bar{q}q\rangle$ on $\theta = \mu_{\rm I}/T$. We introduce a dual parameter for the deconfinement transition by making use of this dependence. By changing a four-fermion coupling constant, we tune the location of the critical endpoint of the deconfinement transition.

DOI:10.5506/APhysPolBSupp.5.803
PACS numbers: 11.30.Rd, 12.38.Aw, 12.39.Fe, 25.75.Nq

1. Introduction

Phase transitions in QCD have been extensively studied in lattice quantum chromodynamics. While recent development enables us to perform numerical simulations at physical quark masses, which revealed a crossover nature of the QCD phase transition at finite temperature [1], analyses at nonzero quark chemical potential μ have been limited to small μ region due to the complex fermion determinant, known as the "sign problem" [2]. One

* Talk presented at HIC for FAIR Workshop and XXVIII Max Born Symposium "Three Days on Quarkyonic Island", Wrocław, Poland, May 19–21, 2011.

of several methods circumventing this problem is to use an imaginary chemical potential $\mu = i\mu_{\rm I}$. Indeed, this method has provided transition lines in the T–μ plane via an analytic continuation from those obtained at imaginary μ [3,4,5]. Moreover, it has been known that there is a phase transition specific to the imaginary chemical potential characterizing the deconfinement phase at high temperature [6]. Rich phase structures later found in the lattice simulations provide a testing ground for understanding the nature of phase transitions in QCD [7,8,9,10]. Those properties give constraints on model studies which can be extended to real μ. In this work, we study the phase structure of the Polyakov-loop extended Nambu–Jona-Lasinio (PNJL) model [11,13] which satisfies fundamental symmetries of QCD relevant for phase transitions at imaginary chemical potential. Focusing on the deconfinement transition, we show that the "statistical confinement" feature of the model naturally leads to characteristic behaviors of the order parameters while details depend on the choice of the Polyakov loop potential. We discuss dual parameters to characterize the phase transitions. Finally, we point out the existence of the critical endpoint (CEP) associated with the deconfinement transition at imaginary chemical potential and clarify the relation between its location and the chiral phase transition.

In the next section, we will give a brief introduction of the model. We will discuss the characteristic behavior of the order parameters as well as the dual parameters in Sec. 3. The critical endpoint of the deconfinement transition will be discussed in Sec. 4 and Sec. 5 is devoted to the summary. More details can be found in Ref. [14].

2. PNJL model at imaginary chemical potential

The Lagrangian of the two-flavor PNJL model is given by

$$\mathcal{L} = \bar{q}(i\gamma_\mu D^\mu - m_0)q + G_s\left[(\bar{q}q)^2 + (\bar{q}i\gamma_5\vec{\tau}q)^2\right] - \mathcal{U}(\Phi[A], \Phi^*[A]; T)\,. \quad (1)$$

The model is an extension of the NJL model, which is an effective model of chiral properties of QCD [15,16], such that quarks couple with background gluonic fields described by a Z(3) symmetric effective potential $\mathcal{U}$ which takes care of confinement. In the covariant derivative $D^\mu = \partial^\mu - iA^\mu$, only the temporal components of $A_0 = gA_0^a\lambda^a/2$ is included. The effective potential $\mathcal{U}$ is expressed in terms of the traced Polyakov loop and its conjugate, $\Phi = \langle {\rm Tr}_c L\rangle/3$ and $\Phi^* = \langle {\rm Tr}_c L^\dagger\rangle/3$, respectively. This coupling between quarks and gluons leads to an almost simultaneous crossover of the chiral and deconfinement transitions at finite temperature, of which order parameters are chiral condensate $\sigma \equiv \langle\bar{q}q\rangle$ and the Polyakov loop Φ [11], provided the Polyakov loop potential $\mathcal{U}$ yields a first order transition at $T_0 = 270\,{\rm MeV}$ in accordance with pure SU(3) lattice calculations. Two

functional forms of $\mathcal{U}$, which reproduce the thermodynamic quantities obtained in pure SU(3) lattice gauge theory [12], have been used. One has a polynomial form

$$\frac{\mathcal{U}_{\rm Pol}}{T^4} = -\frac{b_2(T)}{2}\Phi^*\Phi - \frac{b_3}{6}\left[\Phi^3 + (\Phi^*)^3\right] + \frac{b_4}{4}(\Phi^*\Phi)^4 \tag{2}$$

with a set of parameters given in [13]. The other is a logarithmic one [17]

$$\frac{\mathcal{U}_{\rm log}}{T^4} = -\frac{a(T)}{2}\Phi^*\Phi + b(T)\log\left\{1 - 6\Phi^*\Phi + 4\left[\Phi^3 + (\Phi^*)^3\right] - 3(\Phi^*\Phi)^2\right\} . \tag{3}$$

The logarithm restricts possible values of Φ and Φ^* to the so-called target space, since the argument of the logarithm must be positive.

At imaginary μ, the two Polyakov loop variables Φ and Φ^* are complex conjugate [18]. Moreover, the partition function of the PNJL model at imaginary chemical potential has been shown [18] to have the same periodicity in $\theta = \mu_{\rm I}/T$ as that of QCD, $\mathrm{Z}(\theta + 2\pi/3) = \mathrm{Z}(\theta)$, which was pointed out by Roberge and Weiss [6] as a remnant of Z(3) symmetry. Therefore, we may express them by using a modulus and a phase $\Phi = |\Phi|e^{i\phi}$ and $\Phi^* = |\Phi|e^{-i\phi}$.

The thermodynamic potential in the mean field approximation reads

$$\begin{aligned}\Omega(T,V,\theta) = \left(G_s\sigma^2 + \mathcal{U}\right)V - 4V\int\frac{d^3p}{(2\pi)^3}\Big[3\left(E_p - E_p^0\right) \\ + T\ln\left[1+3|\Phi|e^{i(\theta+\phi)-\beta E_p}+3|\Phi|e^{i(2\theta-\phi)-2\beta E_p}+e^{3i\theta-3\beta E_p}\right] \\ + T\ln\left[1+3|\Phi|e^{-i(\theta+\phi)-\beta E_p}+3|\Phi|e^{i(\phi-2\theta)-2\beta E_p}+e^{-3i\theta-3\beta E_p}\right]\Big] ,\end{aligned} \tag{4}$$

where $E_p = \sqrt{p^2+M^2}$, $E_p^0 = \sqrt{p^2+m_0^2}$, and $M = m_0 - 2G_s\sigma$. The first term in the momentum integral is a divergent vacuum term, which is regularized by a three-momentum cutoff Λ. The cutoff and coupling are fixed to $G_s = 5.498\,\mathrm{GeV}^{-2}$ and $\Lambda = 0.6315\,\mathrm{GeV}$ so as to reproduce the vacuum pion mass and pion decay constant with $m_0 = 5.5\,\mathrm{MeV}$. In the following, we mainly focus on the result in the chiral limit $m_0 = 0$ to preserve the chiral symmetry in the Lagrangian. The chiral condensate σ serves as an order parameter for the chiral phase transition. The order parameters are determined by the minimum of the potential which is obtained by solving the gap equation $\partial\Omega/\partial X_i = 0$ with $X_i = M, |\Phi|, \phi$.

3. Behavior of the order parameters

3.1. Order parameters at imaginary chemical potential

First, we consider two extreme limits in order to see characteristic θ dependences of σ which has the same periodicity $2\pi/3$ as Ω. Expanding Eq. (4)

for small $e^{-\beta E_p}$, we have a gap equation at small $|\Phi|$ limit in which only a term proportional to $\cos 3\theta$ remains with a small magnitude $\sim e^{-3\beta E_p}$ indicating the statistical confinement. This dependence naturally leads to the periodicity $2\pi/3$ when $|\Phi|$ is negligible and chiral symmetry is broken. On the other hand, when $|\Phi| \simeq 1$, the model reduces to the NJL model except for the coupling of ϕ with θ, as seen in Eq. (4). In this case, the apparent θ dependence is governed by $\cos\theta$ as a consequence of deconfinement. Although this factor does not match with the required periodicity $2\pi/3$, it is preserved by a change of ϕ, namely, the Roberge–Weiss transition.

We show the chiral condensate in the left panel of Fig. 1 obtained by numerically solving the gap equations. One sees that σ at low temperature ($T = 220\,\mathrm{MeV}$) exhibits small and smooth variation as a function of θ, as discussed above. On the other hand, one sees a cusp at $\theta = \pi/3$ and $T = 280\,\mathrm{MeV}$. This is a consequence of a Roberge–Weiss transition depicted in the right panel of Fig. 1, in which the phase ϕ changes from 0 to $-2\pi/3$, smoothly at low T but discontinuously at high T. As a result, the required periodicity of σ is preserved. One also sees a second order chiral phase transition for $T = 280\,\mathrm{MeV}$ in which the chiral symmetry is broken around $\theta = \pi/3$. This implies the chiral critical temperature at imaginary μ is higher than that of zero and real μ. This can be also understood from the gap equation for σ, since $\cos n\theta$ is replaced by $\cosh n\beta\mu$ for real μ.

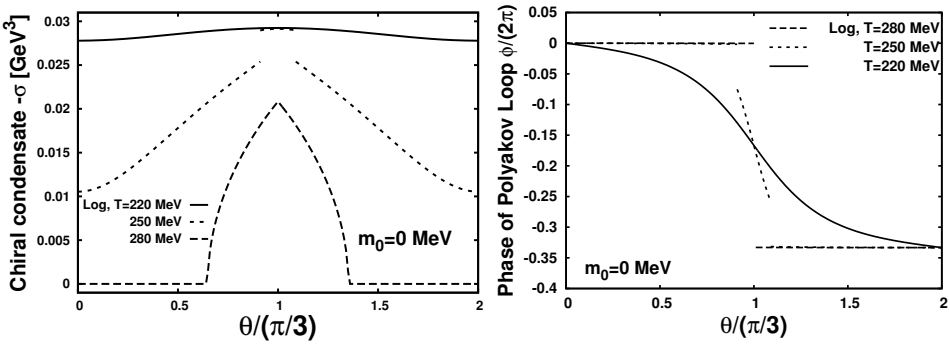


Fig. 1. Left: Chiral condensate for various temperatures as functions of θ. Right: Phase of the Polyakov loop ϕ. Both results are in the chiral limit $m_0 = 0$ and for the logarithmic potential.

While the above properties are independent of the choice of $\mathcal{U}$, there are some potential dependent features as follows. In Fig. 1 and the left panel of Fig. 2, one sees a discontinuity in the order parameters at the same θ. This shows a first order deconfinement transition which exists only in the case of the logarithmic potential (3). The polynomial potential (2) exhibits smoother change near phase transition. In the right panel of Fig. 2, the

target space of the Polyakov loop is displayed. Owing to the Z(3) symmetry, $\mathcal{U}$ has three degenerate minima at $T > T_0$. Putting quarks into the system makes one of those minima favored. While $\mathrm{Im}\Phi = 0$ is always chosen at $\theta = 0$, $\mathrm{Im}\Phi \neq 0$ is favored at imaginary chemical potential due to the coupling of θ and ϕ seen in Eq. (4). At low temperature, where minimum of $\mathcal{U}$ is close to the origin, the minimum of the effective potential smoothly moves from $\phi = 0$ to $\phi = -2\pi/3$ across $\theta = \pi/3$. At high temperature, however, there is a potential wall which makes the transition from point A to point B discontinuous. Since the polynomial potential does not have any restriction of the target space, the minimum passes outside (C) the target space near the RW transition.

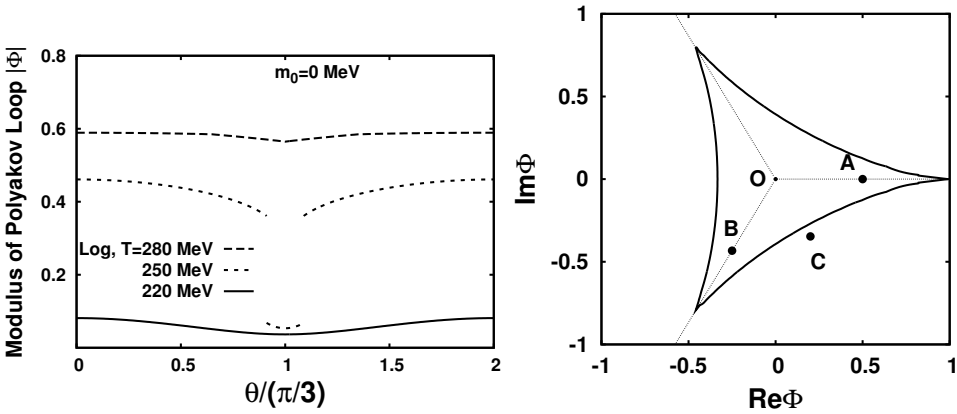


Fig. 2. Left: Modulus of the Polyakov loop $|\Phi|$. Right: Target space of the Polyakov loop on complex Φ plane. A region inside the solid lines denote the target space of the logarithmic potential in which the argument of the logarithm is positive.

The phase diagrams shown in Fig. 3 summarize the behavior of the order parameters. One sees a first order deconfinement transition and an associated critical endpoint (CEP) only for the logarithmic potential. This also implies that the RW endpoint, where the first order RW transition terminates, is a triple point. On the other hand, one sees a second order RW endpoint for the polynomial potential. The properties of the RW endpoint in QCD might reflect the nature of the QCD phase transition at real μ. We refer to Refs. [8] and [7] for recent calculations of $N_f = 2$ and $N_f = 3$ lattice QCD, respectively. Especially, it should be noted that the order of the RW endpoint has a non-trivial bare quark mass dependence which cannot be reproduced by chiral effective models (see Sec. 4). An improved model was proposed in Ref. [19] to reproduce this property.

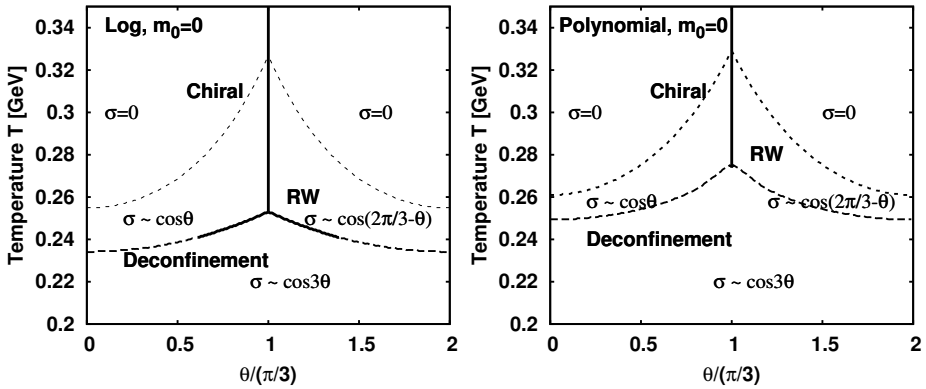


Fig. 3. Phase diagram on T–θ plane. Solid lines, dotted lines, and dashed lines stand for first, second, and crossover transitions, respectively.

3.2. Dual parameters for deconfinement

It has been shown that information on the deconfinement is encoded in θ dependence of σ. We can consider dual parameters which characterize the deconfinement transition. A dual parameter was introduced in [20]. By considering a twisted boundary condition for quarks $q(\boldsymbol{x}, \beta) = e^{i\varphi} q(\boldsymbol{x}, 0)$, one may define the corresponding chiral condensate $\sigma(\varphi)$. Then the dual chiral condensate $\Sigma^{(n)}$ reads

$$\Sigma^{(n)}(T) = -\int_0^{2\pi} \frac{d\varphi}{2\pi} e^{-in\varphi} \left[-\frac{1}{V} \left\langle \mathrm{Tr} \left[(m_0 + D_\varphi)^{-1} \right] \right\rangle \right] . \tag{5}$$

While the twisted boundary condition is similar to introducing imaginary chemical potential [21], it does not apply to the background gauge field. Therefore, $\sigma(\varphi)$ has a periodicity 2π and was calculated in a PNJL model by fixing the Polyakov loop at its $\theta = 0$ value [22]. Particularly $\Sigma^{(1)}$ is called dressed Polyakov loop, since it has the same transformation properties under Z(3) and thus is expected to serve as an order parameter of the deconfinement transition. Analogously, we consider a modified dual parameter which utilizes the characteristic property of $\sigma(\theta)$,

$$\Sigma_\theta^{(n)}(T) = \frac{3}{2\pi} \int_{-\pi/3}^{\pi/3} d\theta e^{-in\theta} \sigma(T, \theta) \, , \tag{6}$$

where we take the integration range $[-\pi/3, \pi/3]$, owing to the periodicity of $\sigma(\theta)$.

We compare those dual parameters for $n = 1$ with the Polyakov loop in Fig. 4, as well as their derivatives with respect to temperature, of which peaks can be regarded as (pseudo)critical temperatures. One sees that while dual parameters show a rapid increase as seen in the Polyakov loop (top)[1], their derivatives exhibit different peak structures. The derivatives of the dual parameters have a peak at the chiral transition temperature, independent of $\mathcal{U}$. As for the deconfinement, however, existence of the peak depends on $\mathcal{U}$. The dressed Polyakov loop exhibits a peak for the $\mathcal{U}_{\rm log}$ for which $|\Phi|$ shows stronger crossover than $\mathcal{U}_{\rm Pol}$. Moreover, the modified dual parameter exhibits only a shoulder even for $\mathcal{U}_{\rm log}$. This result indicates different sensitivity of the dual parameters to the chiral and deconfinement transition.

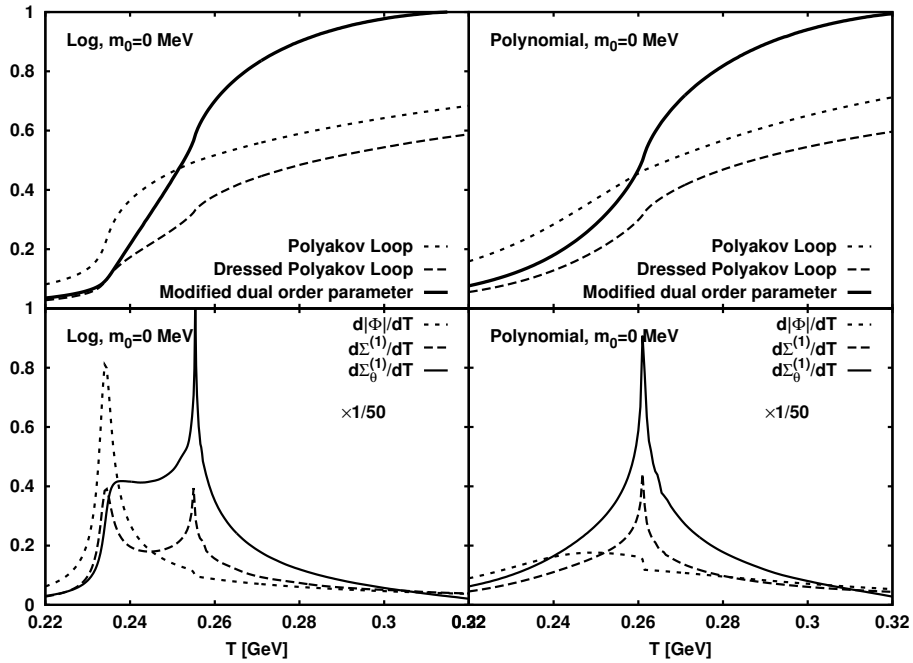


Fig. 4. Dual parameters compared with Polyakov loop. Top panels show Φ, $\Sigma^{(1)}$ and $\Sigma_\theta^{(1)}$ for $\mathcal{U}_{\rm log}$ (left) and $\mathcal{U}_{\rm Pol}$ (right) while bottom ones displays their derivatives with respect to temperature.

4. Critical endpoint of deconfinement

Now, let us turn to the deconfinement CEP found in the case of $\mathcal{U}_{\rm log}$. Here, we vary the four-fermion coupling constant G_s to preserve the chiral symmetry in the Lagrangian. Locations of the CEP are shown in the left of

[1] Dual parameters are normalized to 0 as $T \to 0$ and 1 as $T \to \infty$ [14].

Fig. 5 for various values of G_s. One sees the squared critical chemical potential $\mu^2_{\rm CEP}$ increases with G_s to reach $\mu^2_{\rm CEP} = 0$ around $G_s \simeq 6.3\,{\rm GeV}^{-2}$. In the right of Fig. 5, we also depict a phase diagram for $G_s = 6.5\,{\rm GeV}^{-2}$ in which the CEP exists at real chemical potential. One sees that the first order deconfinement transition starting from the RW endpoint (see Fig. 3) is prolonged, while the chiral critical line moves upward. The relation between these two changes can be understood as follows. Since the Polyakov loop potential $\mathcal{U}_{\rm log}$ has a first order phase transition at $T = T_0$, the model results in the same transition when the effects of quarks are negligible in thermodynamics. The contribution of quarks to thermodynamic potential is essentially determined by the dynamical quark mass $M = m_0 - 2G_s\sigma$, not by the current quark mass m_0, as seen in Eq. (4). When dynamical quark mass becomes lighter, around $T = T_0$, the deconfinement transition is modified to a crossover one. As G_s increases, the stronger coupling leads to a larger condensate $|\sigma(T = 0)|$ thus the dynamical quark mass becomes heavier. This appears as the modified chiral critical line in the phase diagram at $G_s = 6.5\,{\rm GeV}^{-2}$ and the resultant dynamical quark mass is heavy enough to recover the first order the deconfinement transition. At the reference value of G_s, the imaginary chemical potential weakens the thermal terms by $\cos n\theta$ in the thermodynamic potential thus resembling a heavier quark mass which yields the CEP and a first order transition. While the above consideration is completely independent of the form of $\mathcal{U}$, quantitative features such as the value of dynamical quark mass which makes the transition first order depend on the choice of $\mathcal{U}$.

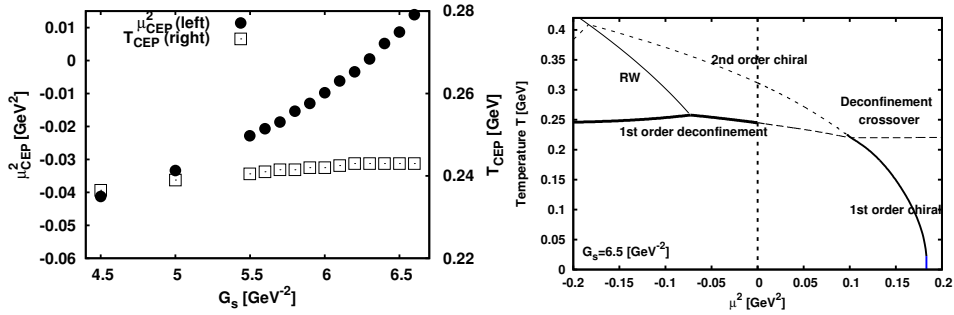


Fig. 5. Left: Location of the deconfinement CEP $(T_{\rm CEP}, \mu^2_{\rm CEP})$ as a function of G_s. Right: Phase diagram for $G_s = 6.5\,{\rm GeV}^{-2}$ which gives $\mu^2_{\rm CEP} > 0$.

Figure 6 shows the behavior of $|\Phi|$ for various G_s at vanishing chemical potential. One sees that $|\Phi|$ becomes steeper for larger G_s in both of $\mathcal{U}$. The case of $\mathcal{U}_{\rm log}$ has a discontinuity already at $G_s = 6.5\,{\rm GeV}^{-2}$ as mentioned above. $\mathcal{U}_{\rm Pol}$, which has a smoother variation of $|\Phi|$ against T, eventually approaches the pure gauge case for much larger G_s. At $G_s = 25\,{\rm GeV}^{-2}$,

where the dynamical quark mass at $T = 0$ is around 2.5 GeV, the first order deconfinement transition is recovered. The origin of this difference is the much weaker first order transition in $\mathcal{U}_{\rm Pol}$, which easily turns into crossover when quarks heavier than 2.5 GeV are put into the system. If one characterizes a strength of the deconfinement transition by a gap of the Polyakov loop $\Delta\Phi$ at $T = T_0$, one finds $\Delta\Phi = 0.47$ for $\mathcal{U}_{\rm log}$ and 0.072 for $\mathcal{U}_{\rm Pol}$. Since G_s determines the scale of the dynamical chiral symmetry breaking, $\sigma(T = 0)$, this result indicates an interplay of the two transitions which have a unique scale, $\Lambda_{\rm QCD}$, in the case of QCD.

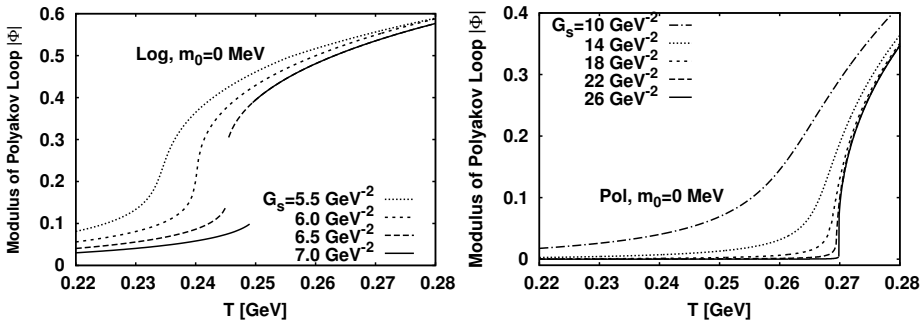


Fig. 6. Behavior of $|\Phi|$ for large G_s. Left: $\mathcal{U}_{\rm log}$. Right: $\mathcal{U}_{\rm Pol}$.

It has been shown that a first order deconfinement phase transition also emerges in the large N_c limit of the PNJL model [23]. This result has a common origin with the present study in a sense that taking large N_c limit makes the system gluon dominated due to $1/N_c$ suppression of the quark contribution, while large G_s thermally suppresses quarks in the chirally broken phase. In our case, however, chiral transition temperature moves upward, thus, there is a discrepancy between the deconfinement and chiral transition temperatures, in contrast to the large N_c limit with a fixed $G_s N_c$ in [23].

5. Summary

We have explored the deconfinement transition in the PNJL model at imaginary chemical potential. We point out that the chiral condensate at imaginary chemical potential, $\sigma(\theta)$, has a characteristic θ dependence due to the deconfinement property which naturally arises from the statistical confinement feature of the model. While the confined phase is characterized by a smooth $\cos 3\theta$ dependence, the deconfined phase exhibits $\cos\theta$ dependence together with cusps at $\theta = \pi/3 \pmod{2\pi/3}$ induced by the abrupt change of the phase of the Polyakov loop (Roberge–Weiss transition). We introduce a new dual parameter utilizing this θ dependence and compare it with the Polyakov loop and the dressed Polyakov loop. Different sensitivities of these

parameters to chiral and deconfinement transitions are found. Changing the four fermion coupling constant, we found that an interplay between the thermal quark contribution through the dynamical chiral symmetry breaking and the Polyakov loop potential determines the location of the deconfinement CEP at imaginary chemical potential. In particular, we found that the deconfinement CEP can be located in the real chemical potential regime for a Polyakov loop potential with a strong first order transition and large dynamical chiral symmetry breaking. We expect that these results are useful for understanding of the QCD phase transition.

This work is supported by the Yukawa International Program for Quark-Hadron Sciences at Kyoto University. K.M. and V.S. acknowledge FIAS for support. B.F. and K.R. acknowledge partial support by EMMI. K.R. acknowledges partial support by the Polish Ministry of Science and Higher Education (MNiSW). V.S. was supported by the U.S. Department of Energy under Contract No. DE-AC02-98CH10886.

REFERENCES

[1] Y. Aoki *et al.*, *Nature* **443**, 675 (2006); A. Bazavov *et al.*, *Phys. Rev.* **D85**, 054503 (2012) [arXiv:1111.1710v2].

[2] S. Muroya, A. Nakamura, C. Nonaka, T. Takaishi, *Prog. Theor. Phys.* **110**, 615 (2003).

[3] P. de Forcrand, O. Philipsen, *Nucl. Phys.* **B642**, 290 (2002); *Nucl. Phys.* **B673**, 170 (2003); *J. High. Energy Phys.* **01**, 077 (2007).

[4] M. D'Elia, M.P. Lombardo, *Phys. Rev.* **D67**, 014505 (2003); *Phys. Rev.* **D70**, 074509 (2004).

[5] M. D'Elia, F.D. Renzo, M.P. Lombardo, *Phys. Rev.* **D76**, 114509 (2007).

[6] A. Roberge, N. Weiss, *Nucl. Phys.* **B275**, 734 (1986).

[7] P. de Forcrand, O. Philipsen, *Phys. Rev. Lett.* **105**, 152001 (2010).

[8] M. D'Elia, F. Sanfilippo, *Phys. Rev.* **D80**, 111501(R) (2009); C. Bonati, G. Cossu, M. D'Elia, F. Sanfilippo, *Phys. Rev.* **D83**, 054505 (2011).

[9] H.S. Chen, X.Q. Luo, *Phys. Rev.* **D72**, 034504 (2005); L.K. Wu, X.Q. Luo, H.S. Chen, *Phys. Rev.* **D76**, 034505 (2007).

[10] K. Nagata, A. Nakamura, *Phys. Rev.* **D83**, 114507 (2011).

[11] K. Fukushima, *Phys. Lett.* **B591**, 277 (2004).

[12] G. Boyd *et al.*, *Nucl. Phys.* **B469**, 419 (1996).

[13] C. Ratti, M.A. Thaler, W. Weise, *Phys. Rev.* **D73**, 014019 (2006).

[14] K. Morita, V. Skokov, B. Friman, K. Redlich, *Phys. Rev.* **D84**, 076009 (2011).

[15] Y. Nambu, G. Jona-Lasinio, *Phys. Rev.* **122**, 345 (1961); *Phys. Rev.* **124**, 246 (1961).

[16] T. Hatsuda, T. Kunihiro, *Phys. Rep.* **247**, 221 (1994).

[17] S. Roessner, C. Ratti, W. Weise, *Phys. Rev.* **D75**, 034007 (2007).

[18] Y. Sakai, K. Kashiwa, H. Kouno, M. Yahiro, *Phys. Rev.* **D77**, 051901(R) (2008).

[19] Y. Sakai, T. Sasaki, H. Kouno, M. Yahiro, *Phys. Rev.* **D82**, 076003 (2010).

[20] E. Bilgici, F. Bruckmann, C. Gattringer, C. Hagen, *Phys. Rev.* **D77**, 094007 (2008).

[21] N. Weiss, *Phys. Rev.* **D35**, 2495 (1987).

[22] K. Kashiwa, H. Kouno, M. Yahiro, *Phys. Rev.* **D80**, 117901 (2009).

[23] L. McLerran, K. Redlich, C. Sasaki, *Nucl. Phys.* **A824**, 86 (2009).